

© 2018 IEEE. Personal use of this material is permitted. Permission from IEEE must be obtained for all other uses, in any current or future media, including reprinting/republishing this material for advertising or promotional purposes, creating new collective works, for resale or redistribution to servers or lists, or reuse of any copyrighted component of this work in other works.

Conference: 2019 Joint MMM-Intermag Conference, Washington DC, 14 - 18 Jan 2019

DOI: 10.1109/TMAG.2018.2885434.

URL: <http://ieeexplore.ieee.org/stamp/stamp.jsp?tp=&arnumber=8587131&isnumber=4479871>

Viscoelastic Lubricant Deformation and Disk-to-Head Transfer during Heat-Assisted Magnetic Recording (HAMR)

Siddhesh V. Sakhalkar¹, David B. Bogy¹, *Life Fellow, IEEE*

¹ Department of Mechanical Engineering, University of California, Berkeley, CA 94720, USA

One of the challenges in Heat-Assisted Magnetic Recording (HAMR) is the formation of write-induced head contamination at the near field transducer. A possible mechanism that has been proposed for this contamination is the transfer of lubricant from the disk to the head due to temperature driven evaporation/condensation. Most previous studies on lubricant depletion due to laser heating have assumed the lubricant to be a viscous fluid and have modeled its behavior using traditional lubrication theory. However, Perfluoropolyether (PFPE) lubricants are viscoelastic fluids and are expected to exhibit a combination of viscous and elastic behavior at the time and length scales of HAMR conditions. In this study, we use a modified Reynolds lubrication equation for the viscoelastic fluid that employs the Linear Maxwell constitutive model. We use this modified lubrication equation to develop a model that predicts the disk-to-head lubricant transfer during HAMR writing. This model simultaneously determines the thermo-capillary stress driven deformation and evaporation of the viscoelastic lubricant film on the disk, the diffusion of the vapor phase lubricant in the air bearing and the evolution of the condensed lubricant film on the head. We investigate the effects of lubricant type (Zdol vs Ztetraol), head/disk temperature, initial lubricant thickness and laser spot size on the lubricant transfer process. Simulation results show a significant difference between the rates of transfer for Zdol (timescale of ns) versus Ztetraol (timescale of μ s). The amount of transfer increases with the disk temperature and the initial lubricant thickness.

Index Terms—Hard Disk Drives, Heat-Assisted Magnetic Recording (HAMR), Lubricant, Viscoelasticity, Contamination, Smear

I. INTRODUCTION

RELIABILITY of the head-disk interface (HDI) during high temperature laser heating still remains a major challenge that needs to be addressed before Heat-Assisted Magnetic Recording (HAMR) can be made into a robust commercial product. One of the challenges in HAMR is the formation of write-induced head contamination at the near field transducer (NFT). Kiely et al. [1] reported that head contamination begins soon after the laser is turned on and grows over time until the contamination height reaches the head-disk clearance. Once the head contamination contacts the media surface, the disk motion generates a smear down-track of the NFT. One possible mechanism for this contamination is lubricant transfer from the disk to the head through thermodynamic driving forces [1], [2]. During HAMR, the media is locally heated to its Curie temperature (~ 500 °C). However, the peak temperature of the head is lower than that of the disk (~ 300 °C) [1]. This temperature difference causes the lubricant to evaporate from the disk and condense on the relatively cooler head. The lubricant acts as a carrier, causing a continuous deposition of media contaminants at the NFT.

Most previous studies have investigated lubricant behavior during HAMR while assuming the lubricant to be a purely viscous material [3], [4]. However, experiments show that PFPE lubricants are viscoelastic fluids [5] and hence can behave like viscous fluids or elastic solids or a combination of both depending on the flow timescale. Sarabi & Bogy studied the effect of viscoelasticity on lubricant behavior under HAMR using a FEM implementation of the Linear Maxwell model in ANSYS [6]. They found that the lubricant exhibits elastic behavior during HAMR with instantaneous deformations.

Understanding the mechanism of media-to-head lubricant and contaminant transfer is crucial in order to eliminate or control its effect and to develop reliable HAMR drives. In our previous study [4], we developed a viscous model that predicts the media-to-head lubricant transfer during HAMR writing for the PFPE lubricant, Zdol. This model simultaneously determines the thermo-capillary stress driven deformation and evaporation of the lubricant film on the disk, the convection and diffusion of the vapor phase lubricant in the air bearing and the evolution of the condensed lubricant film on the slider. However, this model assumes a viscous constitutive law for the lubricant, which in reality is a viscoelastic fluid.

In this study, we use a modified Reynolds lubrication equation for the viscoelastic fluid that employs the Linear Maxwell model. We use this equation to predict the media-to-head lubricant transfer for the viscoelastic lubricant. In reference [7], we also studied rheological effects on lubricant behavior during HAMR. We compared the deformation, recovery and disk-to-head transfer of the viscoelastic lubricant with that for a purely viscous model and additionally investigated the effect of incorporation of a slip boundary condition on the lubricant behavior [7]. In this study, we focus on the effects of HAMR design parameters such as head temperature, media temperature, initial disk lubricant thickness and laser FWHM on the disk-to-head lubricant transfer process for the viscoelastic lubricants, Zdol and Ztetraol.

II. LUBRICANT MODEL

Exposure to HAMR laser heating causes the lubricant on the disk (thickness h_d) to deform and evaporate. Evaporation increases the partial pressure of the lubricant vapor in the air bearing, p_v . Some of this vapor condenses on the head, depositing a film of thickness h_s . We consider two frames of

TABLE I
WLF COEFFICIENTS C_1 , C_2 , VISCOSITY AT GLASS TEMPERATURE T_0 ,
SHEAR MODULUS FOR ZDOL, ZTETRAOL [5]

Lubricant	Zdol 2500	Ztetraol 2000
T_0	-113.6 °C	-112.2 °C
C_1	13.62	23.22
C_2	59.72	45.81
$\eta_{bulk}(T_0)$	4.16 e+8 Pa-s	2.34 e+17 Pa-s
G_{bulk}	51.9 kPa	36.6 kPa

reference: frame 1 - attached to the disk and frame 2 - attached to the slider. In frame 1, the disk is stationary and the head (and the laser spot) move with speed U . In frame 2, the head is stationary and the disk moves backwards with speed U .

A. Lubricant Rheology

The incompressible linear Maxwell model is described by the following equation for the Cauchy stress $\boldsymbol{\sigma}$:

$$\begin{aligned} \boldsymbol{\sigma} &= -p\mathbf{I} + \boldsymbol{\tau} \\ \frac{\boldsymbol{\tau}}{\eta} + \frac{1}{G} \frac{\partial \boldsymbol{\tau}}{\partial t} &= \nabla \mathbf{v} + (\nabla \mathbf{v})^T \end{aligned} \quad (1)$$

Here p is the pressure, $\boldsymbol{\tau}$ is the extra stress and \mathbf{v} is the velocity. The viscosity η and the shear modulus G are related to the Maxwell Relaxation time λ by: $\eta = G\lambda$.

Karis studied bulk rheological properties of PFPE lubricants by measuring their viscosity (η_{bulk}), storage modulus, loss modulus via steady-shear and dynamic oscillation measurements [5]. Accordingly, η_{bulk} can be expressed as a function of temperature using Williams Landel Ferry (WLF) Coefficients:

$$\begin{aligned} \eta_{bulk}(T) &= \eta_{bulk}(T_0) a_{T_0}(T) \\ \log(a_{T_0}) &= \frac{-C_1(T - T_0)}{C_2 + (T - T_0)} \end{aligned} \quad (2)$$

Here reference temperature T_0 is the PFPE glass temperature, C_1 & C_2 are the WLF coefficients with respect to T_0 , $\eta_{bulk}(T_0)$ is the viscosity at T_0 . T_0 , C_1 , C_2 , $\eta(T_0)$, G for Zdol/Ztetraol are given in Table I.

Karis et al. [8] demonstrated that the flow of molecularly thin PFPE films can be described by continuum theory with the adoption of an enhanced effective viscosity. They found a viscosity enhancement factor of ~ 13 for 1 nm thick Zdol 4000. We assume that the effective viscosity for both Zdol and Ztetraol is 13 times the bulk viscosity determined using (2) (i.e. $\eta_{eff} = 13 \times \eta_{bulk}$). Since no quantitative data is available in literature about the effect of confinement on the Maxwell relaxation time, we assume that $G_{eff} = 13 \times G_{bulk}$ and $\lambda_{eff} = \lambda_{bulk}$ [6].

B. Lubrication Theory based on the Linear Maxwell Model

We consider a thin lubricant film of thickness $h(x, y, t)$ on a flat substrate, moving at a constant speed U . The frame of reference is moving along with the substrate (so that the substrate appears to be rest). The co-ordinate system is defined

such that the z axis is along the lubricant thickness and the x axis is along the direction of the substrate velocity. The top surface of the lubricant is free to evolve under the influence of external shear stress $\boldsymbol{\tau}_b(x, y, t) = \tau_{b,x}\mathbf{e}_x + \tau_{b,y}\mathbf{e}_y$ and pressure p . The governing evolution equation for the viscoelastic lubricant using the Linear Maxwell constitutive model (1), according to lubrication theory is:

$$\begin{aligned} \frac{\partial h}{\partial t} + \frac{\partial}{\partial x} \left(-\frac{h^3}{3\eta} \frac{\partial p}{\partial x} + \frac{h^2}{2\eta} \tau_{b,x} \right) \\ + \frac{\partial}{\partial x} \left(-\frac{h^3}{3G} \frac{\partial^2 p}{\partial t \partial x} - \frac{h^2}{2G} \frac{\partial p}{\partial x} \frac{\partial h}{\partial t} + \frac{h^2}{2G} \frac{\partial \tau_{b,x}}{\partial t} \right) \\ + \frac{\partial}{\partial y} \left(-\frac{h^3}{3\eta} \frac{\partial p}{\partial y} + \frac{h^2}{2\eta} \tau_{b,y} \right) \\ + \frac{\partial}{\partial y} \left(-\frac{h^3}{3G} \frac{\partial^2 p}{\partial t \partial y} - \frac{h^2}{2G} \frac{\partial p}{\partial y} \frac{\partial h}{\partial t} + \frac{h^2}{2G} \frac{\partial \tau_{b,y}}{\partial t} \right) \\ + \frac{\dot{m}}{\rho} = 0 \end{aligned} \quad (3)$$

A detailed derivation of (3) can be found in [7].

C. Governing Equation for Disk Lubricant

1) Lubricant Shear Stress

Assuming that surface tension decreases linearly with temperature, the external thermo-capillary shear stress $\boldsymbol{\tau}_b$ in (3) acting on a quasi-parallel film is given by [3]

$$\boldsymbol{\tau}_b = \tau_{b,x}\mathbf{e}_x + \tau_{b,y}\mathbf{e}_y = -c \left(\frac{\partial T_d}{\partial x} \mathbf{e}_x + \frac{\partial T_d}{\partial y} \mathbf{e}_y \right) \quad (4)$$

We assume $c = 0.06 \text{ mN}/(m^\circ\text{C})$ [3]. The disk temperature profile $T_d(x, y, t)$ is assumed to be a Gaussian curve with FWHM of 20 nm, moving with speed U (in frame 1).

2) Lubricant Pressure

Of the normal pressures acting on the lubricant in the HDI (air bearing pressure, disjoining pressure, Laplace pressure), the disjoining pressure has a dominant effect on lubricant evolution during HAMR writing [3]. For lubricants with reactive end groups, the total disjoining pressure has 3 components - van der Waals, electrostatic and structural [9]. However, for thin films, the van der Waals component becomes dominant and thus, pressure p in (3) is given by

$$p = -\frac{A_{VLS}}{6\pi(h_d + d_0)^3} \quad (5)$$

Here $A_{VLS} = 1 \times 10^{-19} \text{ J}$ is the Hamaker constant for the vapor-liquid-solid system; $d_0 = 0.3 \text{ nm}$ [9].

3) Evaporation

The net evaporation rate from the disk $\dot{m} \equiv \dot{m}_d$ in (3) is determined using the following equation: [3]

$$\dot{m}_d = \sqrt{\frac{M_w}{2\pi RT_d}} \left(p_{vap,\infty} \exp\left(-\frac{M_w}{\rho RT_d} \pi(h_d)\right) - p_v \right) \quad (6)$$

Here M_w is the lubricant molecular weight, R is the molar universal gas constant, T_d is the disk lubricant temperature,

$p_{v,\infty}$ is the bulk equilibrium vapor pressure of the lubricant and p_v is the partial pressure of the lubricant vapor in the air bearing. Karis gives the bulk vapor pressure $p_{vap,\infty}$ of Zdol 2000 as a function of temperature using the Clausius-Clapeyron equation [5]. $p_{vap,\infty}$ for Ztetraol is obtained with parameters extracted using the Clausius-Clapeyron equation and the measured data in [10]. This model was used by Jones et. al. [11] to predict lubricant depletion in Ztetraol 2700 and was found to agree well with experiments.

4) Governing Equation

Equation (3) (h replaced by h_d) along with (4), (5), (6) describe the evolution of the disk lubricant height $h_d(x, y, t)$ during HAMR writing in frame 1.

D. Governing Equation for Lubricant Vapor

The governing equation for the lubricant vapor in the air bearing can be obtained by integrating the continuity equation along z and applying Fick's Law of Diffusion: [4]

$$\begin{aligned} \frac{\partial}{\partial t}(\rho_v h_a) + \frac{\partial}{\partial x}(\rho_v q_x) + \frac{\partial}{\partial y}(\rho_v q_y) = \\ \frac{\partial}{\partial x} \left(D h_a \frac{\partial \rho_v}{\partial x} \right) + \frac{\partial}{\partial y} \left(D h_a \frac{\partial \rho_v}{\partial y} \right) + \dot{m}_d + \dot{m}_s \end{aligned} \quad (7)$$

Here, $h_a \equiv (fh - h_s - h_d)$ is the air bearing height where fh is the constant head-disk spacing at the NFT. $q_x \equiv \int_{h_d}^{h_d+h_a} v_{a,x} dz$ and $q_y \equiv \int_{h_d}^{h_d+h_a} v_{a,y} dz$ are the volume flow rates per unit length in the x and y directions, obtained from the air bearing velocity $v_{a,x}$ and $v_{a,y}$ (in frame 1). D is the lubricant vapor diffusivity in air (obtained using the Hirschfelder approximation [5]) and \dot{m}_d and \dot{m}_s are the net evaporation mass fluxes from the disk and slider lubricant films respectively. The lubricant vapor temperature T_v is assumed to be equal to the average of the disk and slider temperatures. The lubricant vapor density ρ_v and partial pressure p_v are related by the ideal gas law.

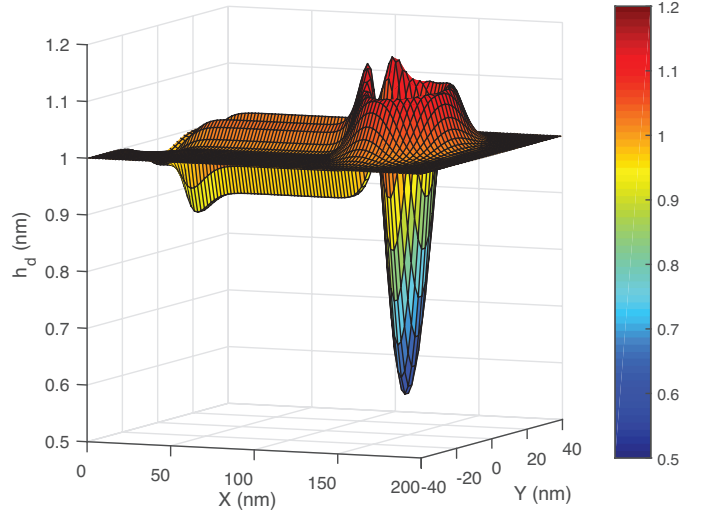
E. Governing Equation for the Slider Lubricant

We solve for the evolution of the lubricant film on the slider in frame 2. In this frame, the slider is stationary and the disk is moving with speed U . The temperature profile of the slider lubricant is a (stationary) Gaussian curve with FWHM of 20 nm. In this frame, the governing equation for the slider lube thickness h_s is again given by (3) (h replaced by h_s).

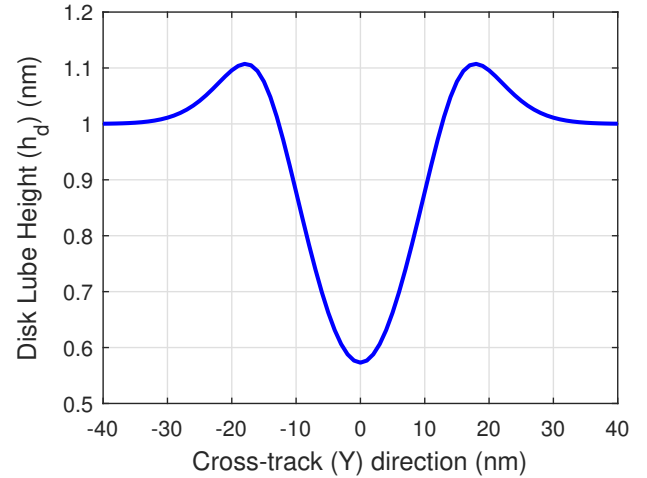
III. RESULTS

A. Viscoelastic Disk Lubricant Deformation

We consider a $h_{0,d} = 1$ nm thick film of Ztetraol on the disk exposed to a scanning laser spot of FWHM 20 nm at 10 m/s. The resultant temperature profile on the disk is assumed to be Gaussian with a peak of 500 °C. Fig. 1a shows a 3D plot of the lubricant profile after 15 ns of laser heating, as seen from frame 1 (stationary disk, moving laser). In this frame, the laser spot is centered at $x = 0$, $y = 0$ at $t = 0$, hence at $t = 15$ ns, the laser spot is at $x = 150$ nm, $y = 0$ nm. The lubricant profile is composed of a trough centered at the instantaneous position of



(a) 3D plot of the disk lubricant profile (h_d)

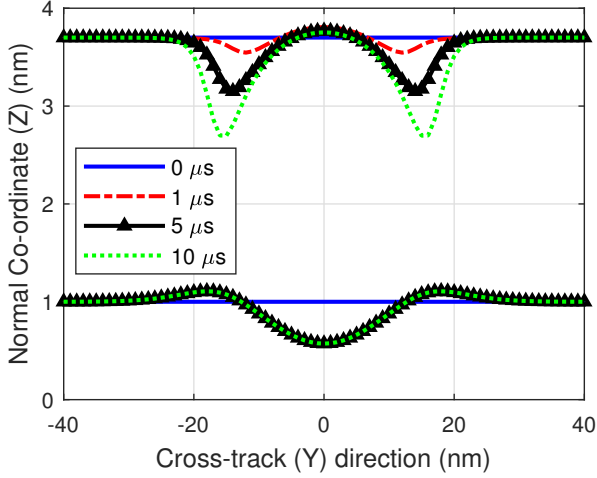


(b) Cross-track disk lubricant profile (at $x = 150$ nm)

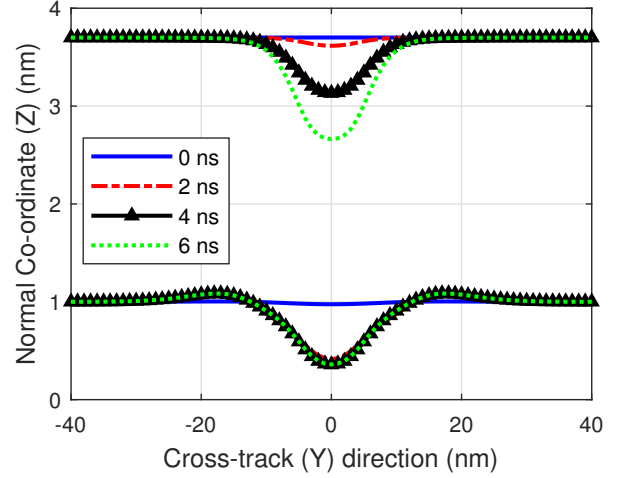
Fig. 1. Disk lubricant profile (Ztetraol) after 15 ns of laser heating. The moving laser spot is centered at $x = 150$ nm, $y = 0$ at $t = 15$ ns in Frame 1. $T_{max,d} = 500$ °C, $U = 10$ m/s, FWHM = 20 nm

the laser spot (i.e. $x = 150$ nm, $y = 0$ nm), with a trail behind it (consistent with results in [7]). As the scanning laser spot moves from $x = 0$ to $x = 150$ nm, the trough follows the laser instantaneously, displaying an elastic behavior. The trail length keeps increasing as the laser moves forward, displaying a viscous behavior. Projection of the lubricant profile along the cross-track (y) direction at $x = 150$ nm is shown in Fig. 1b. Comparison between the profile of this viscoelastic lubricant with a purely viscous model can be found in [7].

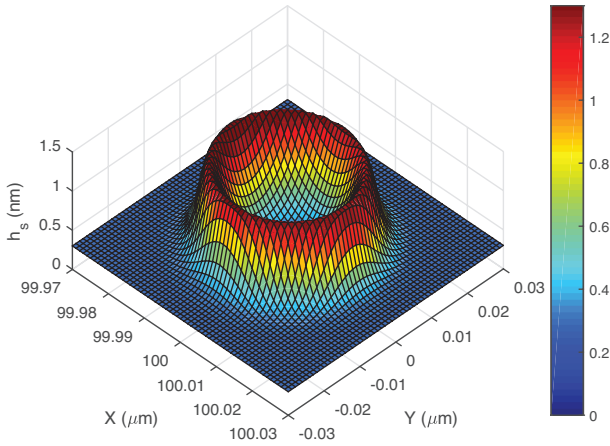
Using (5), the disjoining pressure of a 1 nm thick lubricant film is $\sim 2.4e6$ Pa. On the other hand, the typical value of the Laplace pressure is $\gamma|\nabla^2 h| \sim 1e5$ Pa, where surface tension of the lubricant $\gamma \sim 1e-2$ N/m and maximum value of the Laplacian $|\nabla^2 h| \sim 0.016$ nm⁻¹ for the viscoelastic lubricant profile in Fig. 1a. Hence the Laplace pressure is ignored compared to the disjoining pressure in (5) and (6) in this study.



(a) Disk and slider lubricant profiles in cross-track direction at different times of laser heating for Ztetraol 2700

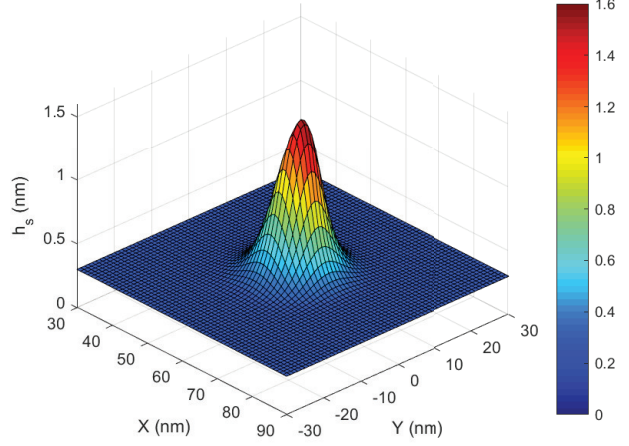


(a) Disk and slider lubricant profiles in cross-track direction at different times of laser heating for Zdol 2000



(b) 3D plot of slider lubricant profile (h_s) after $10 \mu s$ of laser heating. The moving NFT center is located at $x = 100 \mu m$, $y = 0$ at $t = 10 \mu s$ in Frame 1

Fig. 2. Ztetraol 2700 lubricant transfer. $T_{max,d} = 500 \text{ }^\circ C$, $T_{max,s} = 300 \text{ }^\circ C$, $U = 10 \text{ m/s}$, FWHM = 20 nm



(b) 3D plot of slider lubricant profile (h_s) after 6 ns of laser heating. The moving NFT center is located at $x = 60 \text{ nm}$, $y = 0$ at $t = 6 \text{ ns}$ in Frame 1

Fig. 3. Zdol 2000 lubricant transfer. $T_{max,d} = 500 \text{ }^\circ C$, $T_{max,s} = 300 \text{ }^\circ C$, $U = 10 \text{ m/s}$, FWHM = 20 nm

B. Baseline Simulation for Zdol and Ztetraol transfer

We assume an initially uniform film of Zdol 2000/Ztetraol 2700 of thickness $h_{0,d} = 1 \text{ nm}$ on the disk and $h_{0,s} = 0.3 \text{ nm}$ on the head. The disk lubricant is exposed to a scanning laser of FWHM 20 nm at 10 m/s. The peak temperatures of disk and head are $500 \text{ }^\circ C$ and $300 \text{ }^\circ C$ respectively. We apply the initial rise in temperature on the disk/head as a ramp of 2 ns. The head-disk clearance fh is 4 nm. Figs. 2a and 3a show the time evolution of the lubricant profiles on the disk (bottom curves) and the head (top curves) in the cross-track direction for Ztetraol and Zdol respectively. These plots are with respect to frame 1 (stationary disk, moving laser). The moving NFT center/laser spot center is located at $y = 0$ and $x = Ut$ at time t in this frame. The cross-track profiles (lube height vs y) are plotted at $x = Ut$ at time t . We observe a significant difference between the rates of lubricant transfer for Zdol (timescale of ns) vs Ztetraol (time scale of μs). This is due to the difference in vaporization properties of both

lubricants - bulk vapor pressure of Zdol at $500 \text{ }^\circ C$ is 4.9 MPa, while that for Ztetraol is only 2.3 kPa. The shape of the head lubricant profile is also different for both lubricants, as seen in Figs. 2b and 3b. For Zdol, the disk evaporation rate is so high, that condensation of lubricant onto the head dominates over thermo-capillary stress. Hence h_s is maximized at the NFT center, where the disk evaporation rate is maximum (Fig. 3b). On the other hand, with much slower evaporation for Ztetraol, thermo-capillary stress dominates. The condensed lubricant on the slider is pushed away from the NFT center by the thermo-capillary stress, causing lump of accumulated lubricant around a circle centered at NFT, with a radius of $\sim 18 \text{ nm}$ (Fig. 2b). A similar trend in the rates of lubricant transfer for Zdol ($\sim \text{ns}$) vs Ztetraol ($\sim \mu s$) was observed for the generalized viscoelastic model including a slip boundary condition in [7].

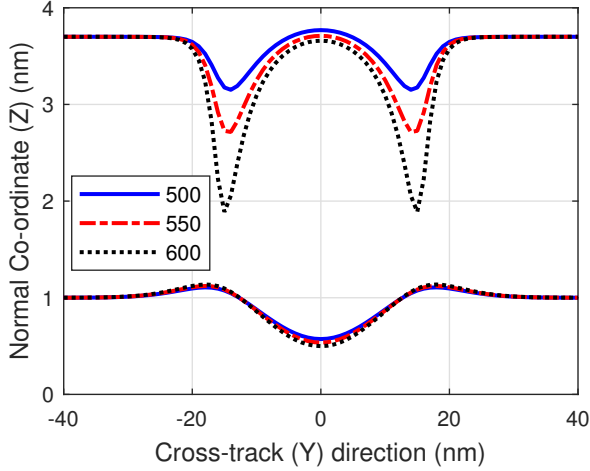


Fig. 4. Disk and slider lubricant profiles in cross-track direction after $5 \mu\text{s}$ of laser heating for Ztetraol 2700. $T_{max,d}$ varied: 500 °C, 550 °C, 600 °C. $T_{max,s} = 300 \text{ °C}$, $U = 10 \text{ m/s}$, FWHM = 20 nm

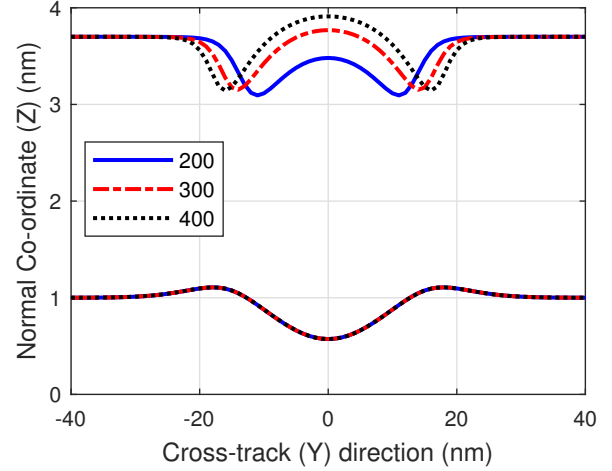


Fig. 5. Disk and slider lubricant profiles in cross-track direction after $5 \mu\text{s}$ of laser heating for Ztetraol 2700. $T_{max,s}$ varied: 200 °C, 300 °C, 400 °C. $T_{max,d} = 500 \text{ °C}$, $U = 10 \text{ m/s}$, FWHM = 20 nm

C. Effect of Media Temperature

In this section, we investigate how lubricant transfer changes with maximum disk temperature, a consequence of varying the laser power. The maximum head temperature is kept constant at 300 °C and the maximum disk temperature is varied: 500 °C, 550 °C and 600 °C. All other parameters are kept fixed (same as Section III-B). Fig. 4 shows the cross-track profiles of the disk and head lubricant thicknesses for the different disk temperatures after $5 \mu\text{s}$ of laser heating for Ztetraol. As the disk temperature increases, the evaporation rate increases, causing the lubricant accumulation on the head to rise. To quantify the increase in lubricant transfer, we record the change in total volume of accumulated lubricant on the slider after $5 \mu\text{s}$ of laser heating. As the disk temperature is increased - 500 °C, 550 °C and 600 °C, the volume of lubricant accumulated on the slider increases significantly - 356 nm^3 , 626 nm^3 and 1010 nm^3 respectively. A similar trend (larger lubricant transfer for higher disk temperature) is expected for Zdol as well [4].

D. Effect of Head Temperature

Next, the maximum disk temperature is kept constant at 500 °C and the maximum slider temperature is varied: 200 °C, 300 °C, 400 °C. All other parameters are kept fixed (same as Section III-B). The resultant cross-track profiles of the disk and head lubricant thicknesses after $5 \mu\text{s}$ of laser heating for Ztetraol are plotted in Fig. 5. We find that change in maximum slider temperature has a relatively small effect on the total amount of lubricant transfer (compared to effect of media temperature). As the head temperature is increased - 200 °C, 300 °C and 400 °C, the volume of lubricant accumulated on the slider decreased only slightly - 369 nm^3 , 356 nm^3 and 345 nm^3 respectively. We do however see a difference in distribution of the accumulated lubricant on the slider in Fig 5. As the head temperature is increased, the thermo-capillary stress on the accumulated lubricant increases, causing

the lubricant to be pushed further away from the NFT center, thereby forming a lump around the NFT. A similar trend (slight decrease in lubricant transfer for higher slider temperature) is expected for Zdol as well [4].

E. Effect of Initial Lubricant Thickness

Here we study how the lubricant transfer process changes with the initial disk lubricant thickness. Fig. 6 shows the cross-track profiles of the disk and head lubricant thicknesses after $5 \mu\text{s}$ of laser heating for three different initial disk lube thicknesses: 0.8, 1 and 1.2 nm for Ztetraol. All other parameters are kept fixed (same as Section III-B). As the disk lubricant thickness is decreased, the lubricant disjoining pressure increases (Refer (5)). The resultant larger disjoining pressure leads to more suppression of the disk evaporation rate (Refer (6)), causing the amount of lubricant transfer to decrease. Accordingly, as the initial disk lubricant thickness is decreased: 1.2 nm, 1 nm, 0.8 nm, the volume of lubricant accumulated on the slider also decreases - 510 nm^3 , 356 nm^3 and 193 nm^3 respectively. A similar trend (larger lubricant transfer for thicker disk lube) is expected for Zdol as well [4].

F. Effect of Laser Spot Size

In this section, we study the effect of laser FWHM on the lubricant transfer process. We plot the disk and slider lubricant profiles in the cross-track direction (normalized by FWHM) for Ztetraol and Zdol for two laser spot sizes: 20 nm and $1 \mu\text{m}$ in Figs. 7 and 8 respectively. All other parameters are kept fixed (same as Section III-B). The relative importance of thermo-capillary stress vs evaporation for lubricant deformation during HAMR depends on its vaporization properties, laser spot size and peak temperature. In our previous study [7], we found that thermocapillary stress dominates at low spot sizes ($\sim 20 \text{ nm}$) and evaporation dominates at higher spot sizes ($\sim 1 \mu\text{m}$) for Ztetraol at $\sim 500 \text{ °C}$. Hence, as the laser spot

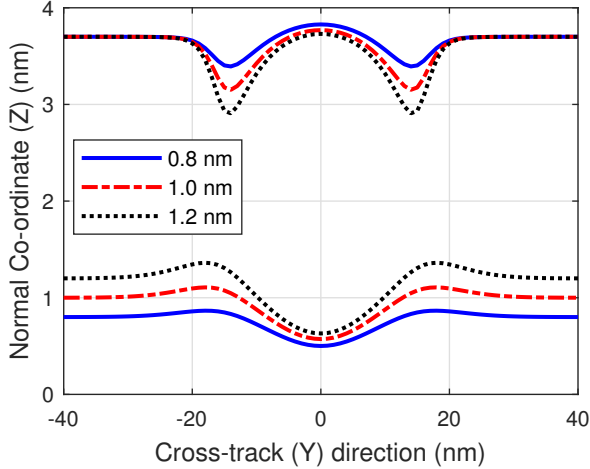


Fig. 6. Disk and slider lubricant profiles in cross-track direction after $5 \mu\text{s}$ of laser heating for Ztetraol 2700. $h_{0,d}$ varied: 0.8 nm, 1 nm, 1.2 nm. $T_{max,d} = 500 \text{ }^\circ\text{C}$, $T_{max,s} = 300 \text{ }^\circ\text{C}$, $U = 10 \text{ m/s}$, FWHM = 20 nm

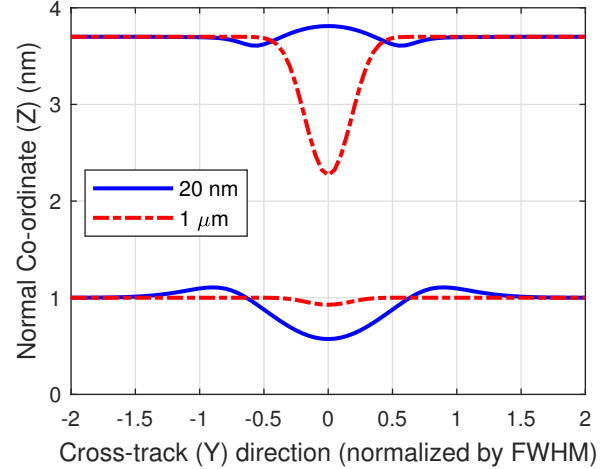


Fig. 7. Disk and slider lubricant profiles in cross-track direction after $0.5 \mu\text{s}$ of laser heating for Ztetraol 2700 for laser FWHM of 20 nm and $1 \mu\text{m}$. $T_{max,d} = 500 \text{ }^\circ\text{C}$, $T_{max,s} = 300 \text{ }^\circ\text{C}$, $U = 10 \text{ m/s}$

size is increased from 20 nm to $1 \mu\text{m}$, the amount of lubricant transfer also increases (Fig. 7). On the other hand, the large vapor pressure of Zdol at $\sim 500 \text{ }^\circ\text{C}$ results in evaporation being the dominant mechanism (over thermocapillary stress) for all spot sizes ($\sim 20 \text{ nm}$ to $1 \mu\text{m}$) [7]. The evaporation rate for Zdol at $\sim 500 \text{ }^\circ\text{C}$ and 20 nm is already so high that increase in laser spot size from 20 nm to $1 \mu\text{m}$ is not very effective in further increasing the evaporation rate (Fig. 8). This is because the lubricant is so thin that the disjoining pressure is extremely large (Refer (5)) and is very effective at suppressing evaporation (Refer (6)).

In order to compare the amount of transfer for different spot sizes, we normalize the volume of lubricant accumulated on the slider (ΔV_{slider}) by the laser FWHM squared: $\overline{\Delta V}_{slider} \equiv \frac{\Delta V_{slider}}{FWHM^2}$ [3]. The resulting length scale $\overline{\Delta V}_{slider}$ for Ztetraol is found to increase from 0.09 nm to 0.25 nm as the spot size is increased from 20 nm to $1 \mu\text{m}$. On the other hand, $\overline{\Delta V}_{slider}$ for Zdol is found to decrease from 0.4 nm and 0.27 nm as the spot size is increased from 20 nm to $1 \mu\text{m}$. This trend of decrease in $\overline{\Delta V}_{slider}$ on increase in FWHM was also observed in our previous viscous simulations for Zdol [4].

G. Lubricant Transfer vs Write-induced Contamination

Media-to-head lubricant transfer is one of the possible mechanisms for write-induced smear on HAMR heads [1]. Contaminants are expected to be a small volumetric percentage of the media lubricant. Hence, contaminants would account for a small fraction of the lube accumulated on the head. This explains why write-induced contamination has been observed to occur on a timescale of seconds [1], even though we predict lubricant transfer to occur on a timescale of μs for Ztetraol.

IV. CONCLUSION

In this study, we have used a modified Reynolds lubrication equation that employs the Linear Maxwell constitutive model to describe the evolution of the viscoelastic lubricant during

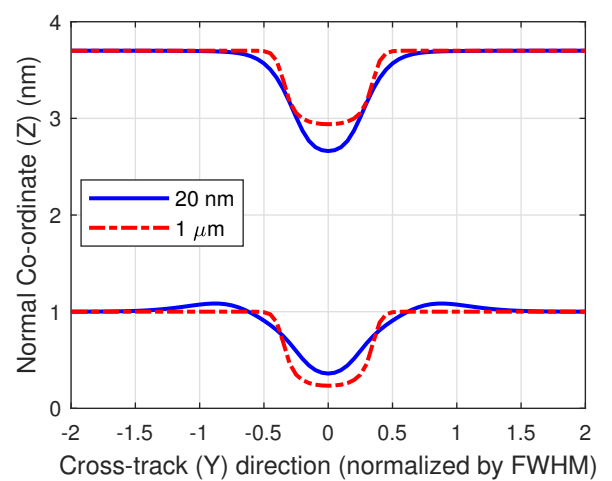


Fig. 8. Disk and slider lubricant profiles in cross-track direction after 6 ns of laser heating for Zdol 2000 for laser FWHM of 20 nm and $1 \mu\text{m}$. $T_{max,d} = 500 \text{ }^\circ\text{C}$, $T_{max,s} = 300 \text{ }^\circ\text{C}$, $U = 10 \text{ m/s}$

HAMR. We have used this equation to predict the media-to-head lubricant transfer during HAMR writing. This model simultaneously determines the thermo-capillary stress driven deformation and evaporation of the viscoelastic lubricant film on the disk, the diffusion of the vapor phase lubricant in the air bearing and the evolution of the condensed lubricant film on the slider. We have investigated the effects of lubricant type, head/media temperature, initial disk lubricant thickness and laser FWHM on the lubricant transfer process. Our results show a significant difference between the rates of transfer for Zdol (timescale of ns) vs Ztetraol (timescale of μs). The amount of transfer increases on increase in media temperature and increase in initial disk lubricant thickness. Comparatively, the head temperature has a small effect on the transfer dynamics. Ztetraol shows larger disk-to-head lubricant transfer for larger spot sizes (on a relative scale). However, Zdol shows smaller transfer for larger spot sizes (on a relative scale).

ACKNOWLEDGMENT

This work was supported by the Computer Mechanics Laboratory at University of California, Berkeley, Mechanical Engineering Department. This is a post-peer-review, pre-copyedit version of an article published in IEEE Transactions on Magnetics. The final authenticated version is available online at: <http://dx.doi.org/10.1109/TMAG.2018.2885434>

Citation for final authenticated version - S. V. Sakhalkar and D. B. Bogy, "Viscoelastic Lubricant Deformation and Disk-to-Head Transfer During Heat-Assisted Magnetic Recording," in IEEE Transactions on Magnetics. doi: 10.1109/TMAG.2018.2885434.

REFERENCES

- [1] Kiely, J.D., Jones, P.M., Y.Yang, Brand, J.L., Anaya-Dufresne, M., Fletcher, P.C., Zavaliche, F., Toivola, Y., Duda, J.C., Johnson, M.T.: "Write-induced head contamination in heat-assisted magnetic recording". *IEEE Trans. Magn.* vol. 53, no. 2, pp. 1-7, Feb. 2017.
- [2] Xiong, S., Wang, N., Smith, R., Li, D., Schreck, E., Dai, Q.: "Material transfer inside head disk interface for heat assisted magnetic recording". *Tribol. Lett.* vol. 65, no. 2, p. 74, Jun. 2017.
- [3] Dahl, J.B., Bogy, D.B.: "Lubricant Flow and Evaporation Model for Heat-Assisted Magnetic Recording Including Functional End-Group Effects and Thin Film Viscosity". *Tribol Lett.* vol. 52, no. 1, pp. 27-45, Oct. 2013.
- [4] Sakhalkar, S.V., Bogy, D.B.: "A Model for Lubricant Transfer from Media to Head During Heat-Assisted Magnetic Recording (HAMR) Writing". *Tribol Lett.* vol. 65, no. 4, p. 166, Dec. 2017.
- [5] Karis, T.: Lubricants for the disk drive industry. In: Rudnick L. (eds) *Lubricant Additives: Chemistry and Applications*, chap 22. CRC Press, Boca Raton, FL, pp. 523584, 2009
- [6] Sarabi, S., Bogy, D.B.: "Effect of Viscoelasticity on Lubricant Behavior Under Heat-Assisted Magnetic Recording Conditions". *Tribol. Lett.* vol. 66, no. 1, p. 33, Mar. 2018.
- [7] Sakhalkar, S.V., Bogy, D.B.: "Effect of Rheology and Slip on Lubricant Deformation and Disk-to-Head Transfer During Heat-Assisted Magnetic Recording (HAMR)". *Tribol. Lett.* vol. 66, no. 4, p. 145, Dec. 2018.
- [8] Karis, T., Marchon, B., Flores, V., Scarpulla, M.: "Lubricant spin-off from magnetic recording disks". *Tribol. Lett.* vol. 11, no. 3/4, pp. 151-159, Nov. 2001.
- [9] Mate, C.M.: Taking a Fresh Look at Disjoining Pressure of Lubricants at Slider-Disk Interfaces. *IEEE Trans. Magn.* vol. 47, no. 1, pp. 124-130, Jan. 2011.
- [10] Solvay-Solexis: Fomblin Z Derivatives: Product Data Sheet. Solvay Solexis, Inc., North America (2002)
- [11] Jones, P.M., Yan, X., Hohlfeld, J., Stirniman, M., Kiely, J.D., Zavaliche, F., Tang, H.H.: "Laser-induced thermo-desorption of perfluoropolyether lubricant from the surface of a heat-assisted magnetic recording disk: lubricant evaporation and diffusion". *Tribol. Lett.* vol. 59, no. 2, p. 33, Aug. 2015.